

Colour-Magnitude Diagrams of Transiting Exoplanets I - Systems with parallaxes

Amaury H. M. J. Triaud^{1,2*}

¹*Kavli Institute for Astrophysics & Space Research, Massachusetts Institute of Technology, Cambridge, MA 02139, USA*

²*Fellow of the Swiss national science foundation*

Accepted ?. Received ?; in original form ?

ABSTRACT

Broadband flux measurements centred around [3.6 μm] and [4.5 μm] obtained with *Spitzer* during the occultation of seven extrasolar planets by their host stars have been combined with parallax measurements to compute the absolute magnitudes of these planets. Those measurements are arranged in two colour-magnitude diagrams. Because most of the targets have sizes and temperatures similar to brown dwarfs, they can be compared to one another. In principle, this should permit inferences about exo-atmospheres based on knowledge acquired by decades of observations of field brown dwarfs and ultra-cool stars' atmospheres. Such diagrams can assemble all measurements gathered so far and will provide help in the preparation of new observational programs. In most cases, planets and brown dwarfs follow similar sequences. HD 2094589b and GJ 436b are found to be outliers, so is the nightside of HD 189733b. The photometric variability associated with the orbital phase of HD 189733b is particularly revealing. The planet exhibits what appears like a spectral type and chemical transition between its day and night sides: HD 189733b straddles the L-T spectral class transition, which would imply different cloud coverage on each hemisphere. Methane absorption could be absent at its hot spot but present over the rest of the planet.

Key words: planetary systems – planets and satellites: atmospheres – binaries: eclipsing – stars: distances – brown dwarfs – Hertzsprung–Russell and colour-magnitude diagrams.

Colour-magnitude diagrams are frequently used in Astronomy to display photometric measurements obtained using different filters. They help identify key features between groups of stars, be it to distinguish different evolutionary stages (e.g. Maeder 1974), or select their spectral types (e.g. Lépine & Gaidos 2011). In addition to direct imaging (Chauvin et al. 2004; Marois et al. 2008), it is possible to measure light re-emitted by an extrasolar planet (Harrington et al. 2006), especially if its orbital inclination produces an occultation (Deming et al. 2005; Seager & Deming 2010). A subset of occulting systems have had their parallax measured by ESA's *Hipparcos* satellite (van Leeuwen 2007). It is therefore possible to obtain accurate absolute magnitudes for transiting extrasolar planets. Combining measurements in several bands, a colour-magnitude diagram can be assembled.

Most planetary flux measurements have been acquired using NASA's *Spitzer* Space Telescope, notably using the IRAC 1 & 2 channels, centred at 3.6 and 4.5 μm (Fazio et al.

2004). These are bands that have frequently been used to observe field brown dwarfs (e.g. Patten et al. 2006) and then combined with parallax measurements, to compile colour-magnitude diagrams (e.g. Dupuy & Liu 2012). Apart from a few, the planets whose flux have been detected fall in the regime of the *hot Jupiters*, whose sizes and temperatures are similar to brown dwarfs'. Both population can therefore be compared to each other.

The aim of this letter is to introduce the first colour-magnitude diagrams for transiting planets using the most accurate distances available so far. This is also an opportunity to showcase the interest of producing such diagrams for exoplanetology.

1 PROCEDURE

Searching the literature (e.g. exoplanets.org; Wright et al. 2011), there are seven systems observed in both [3.6 μm] and [4.5 μm] IRAC channels that also have measured parallaxes in the latest reduction of the *Hipparcos* astrometric data (van Leeuwen 2007). The systems are listed in Table 1.

* E-mail: triaud@mit.edu

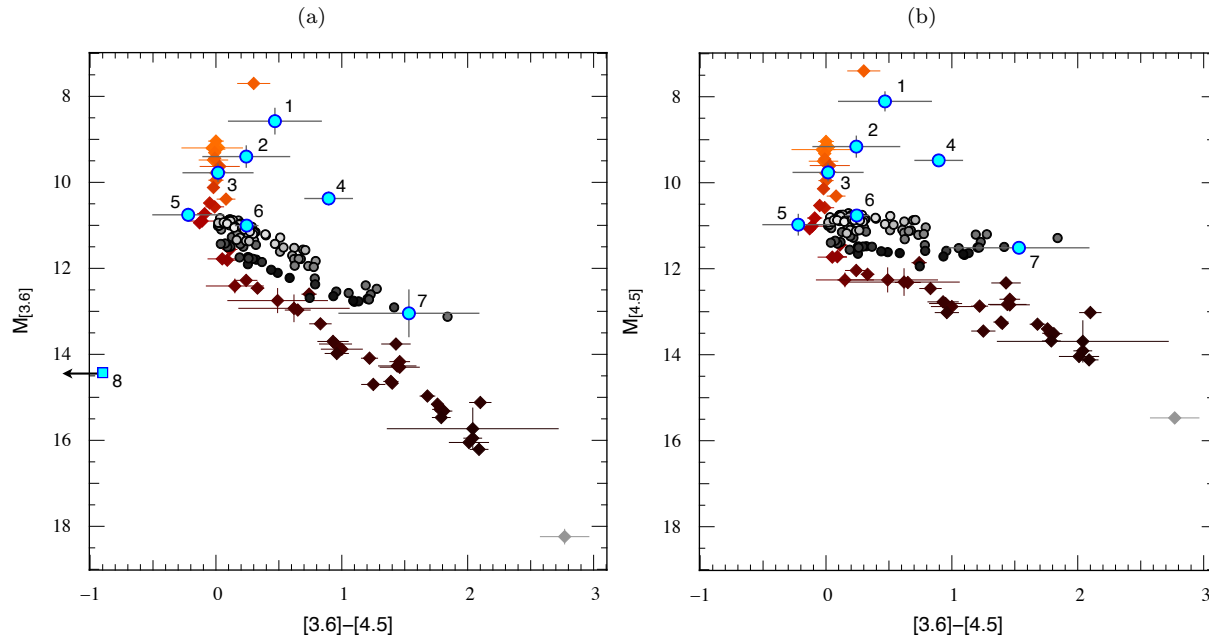


Figure 1. Two colour-magnitude diagrams of absolute magnitudes at $[3.6 \mu\text{m}]$ and $[4.6 \mu\text{m}]$ versus $[3.6]-[4.5]$ colour. The diamonds show late M dwarfs, L, T, and one Y dwarf as compiled in Dupuy & Liu (2012). The grey diamond is WD 0806-661B has no spectral type yet (Luhman et al. 2012). The kink at $M_{[3.6]} \sim 11.5$ corresponds approximately to a L9 spectral type and the location where methane absorption starts appearing in the $[3.6 \mu\text{m}]$ band. Large, blue circles represent the transiting planets whose measurements (and numbers) are located in Table 2. Smaller grey circles represent the phase curve of HD 189733b (Knutson et al. 2012), (lighter gray is for dayside, while darker tones are for nightside). The blue square shows the upper limit of GJ 436b, which is located to the left of the diagram.

All those systems have also been recently observed by NASA’s *WISE* satellite whose W1 and W2 bands are close the IRAC 1 & 2 channels and whose all-sky photometric catalog is readily available (Cutri & et al. 2012). Using parallaxes, absolute magnitudes were computed and errors were propagated (errors are dominated by the uncertainty on the distance, and on the planet’s flux). Results are located in Table 1.

All planetary fluxes were obtained from the published literature and transformed into absolute magnitudes using the standard convention and the values gathered in Table 1. Most measurements are for the dayside emission. The nightside emission in both channels has only been undoubtedly detected for HD 189733b. The planet’s absolute magnitudes are displayed in Table 2. They are plotted in Figure 1, overlaid on field brown dwarfs measurements obtained from Dupuy & Liu (2012). Spectral types range from M6 to Y0, encompassing the L & T classes (Kirkpatrick 2005; Kirkpatrick et al. 2012)

In addition to the flux measurements at superior and inferior conjunctions, Knutson et al. (2012) observed HD 189733b in both IRAC channels during a full orbital phase. Those fluxes have also been converted to absolute magnitudes and binned for visual convenience. They are represented as grey circles. White corresponds to mid-occultation time (midday), and black to mid-transit time (midnight) as seen from Earth. They are to be read clockwise.

Table 2. Absolute magnitudes for the seven extrasolar planet whose hosts have parallaxes. Numbers in the last column correspond to those displayed on Figure 1.

Name		Absolute magnitudes		Refs
		$M_{[3.6]}$	$M_{[4.5]}$	
WASP-33b	day	8.58 ± 0.30	8.11 ± 0.22	1
WASP-18b	day	9.40 ± 0.25	9.16 ± 0.24	2
HAT-P-2b	day	9.78 ± 0.20	9.76 ± 0.19	3
HD 209458b	day	10.38 ± 0.15	9.48 ± 0.12	4
HD 149026b	day	10.76 ± 0.15	10.98 ± 0.24	5
HD 189733b	day	11.006 ± 0.076	10.762 ± 0.045	6
HD 189733b	night	13.06 ± 0.54	11.51 ± 0.12	7
GJ 436b	day	14.42 ± 0.11	> 15.5	8

References: 1) Deming et al. (2012); 2) Knutson et al. (2009); 3) Lewis et al. (2013); 4) Knutson et al. (2008); 5) Maxted et al. (2012); 6-7) Knutson et al. (2012); 8) Stevenson et al. (2010)

2 DISCUSSION

The most striking feature in the $[3.6]-[4.5]$ colour is a *kink* occurring around $M_{[3.6]} \sim M_{[4.5]} \sim 11.5$ which has been interpreted as the emergence of methane absorption in the $[3.6 \mu\text{m}]$ band with decreasing effective temperatures (Patton et al. 2006). This kink occurs as brown dwarfs transition from spectral class L to T (Dupuy & Liu 2012).

The planets’ dayside magnitudes are broadly compatible with the vertical M and L sequence. Two outliers are found: HD 209458b and GJ 436b. Most hot Jupiters are bloated (Charbonneau et al. 2000; Demory & Seager 2011),

Table 1. Apparent WISE 1 & 2 magnitudes and computed absolute magnitudes for the seven occulting planet hosts having parallaxes.

Name	distance (pc)	Apparent magnitudes		Absolute magnitudes	
		W1	W2	$M_{[3.6]}$	$M_{[4.5]}$
GJ 436	10.14 ± 0.24	5.987 ± 0.052	5.703 ± 0.025	5.956 ± 0.071	5.672 ± 0.057
HD 189733	19.45 ± 0.26	5.366 ± 0.065	5.337 ± 0.025	3.921 ± 0.071	3.892 ± 0.038
HD 209458	49.6 ± 2.0	6.287 ± 0.048	6.280 ± 0.022	2.808 ± 0.098	2.801 ± 0.090
HD 149026	79.4 ± 4.4	6.760 ± 0.037	6.804 ± 0.021	2.26 ± 0.13	2.30 ± 0.12
WASP-18	99 ± 11	8.072 ± 0.023	8.116 ± 0.021	3.09 ± 0.23	3.14 ± 0.24
HAT-P-2	114.3 ± 9.8	7.562 ± 0.025	7.583 ± 0.020	2.27 ± 0.18	2.29 ± 0.19
WASP-33	116 ± 11	7.429 ± 0.027	7.455 ± 0.019	2.11 ± 0.20	2.14 ± 0.20

and thus larger than typical brown dwarfs (Díaz et al. 2013; Baraffe et al. 1998; Burrows, Heng & Nampaisarn 2011), even under irradiation (Deleuil et al. 2008; Anderson et al. 2011; Triaud et al. 2013b). A change in radius can lead to a change in luminosity. This would make HD 209458b, ~ 0.9 magnitude brighter and GJ 436b almost 2 magnitudes fainter than a brown dwarf that has the same effective temperature. This simple correction does not explain alone the discrepancy and suggests the need for an additional explanation. HD 209458b’s redder colour may point to different atmospheric behaviour than for brown dwarfs and the majority of hot Jupiters. In the current sample this is the planet with the lowest gravity (Southworth, Wheatley & Sams 2007). GJ 436b is also hard to reconcile and may localise a Neptune-sequence, with different chemistry, of which this is the first example. However it is also possible that both measurements have been affected by systematics. For example, GJ 436b’s [3.6 μ m] dayside flux measurement may have been polluted by stellar variability (Stevenson et al. 2010).

The phase curve of HD 189733b (Knutson et al. 2012) is to be read clockwise. A global offset of the phase curve by -0.5 mag was anticipated due to a radius difference between HD 189733b and typical brown dwarfs. Starting from occultation (6), the planet cools down and follows a slightly shallower slope compared to the T-dwarf sequence. The reason for this is unclear but could lie in the manner heat redistribution is achieved. As the night-side rolls into view the planet progressively returns to the T-dwarf sequence. It follows the kink to finally rise vertically along the L-dwarf sequence reaching climax at $M_{[3.6]} = 11$ mag.

Assuming no chemical alteration, an increase in temperature will cause a vertical increase. At [3.6]-[4.5] = 0.5, there is an offset of about one magnitude between the day and night sides. This corresponds to a temperature ratio of 1.6 between both hemispheres, which is consistent with what has been measured (Knutson et al. 2012).

The dayside emission, at occultation, is slighter fainter and redder than the brightest emission. The fainting has been already interpreted as a hot spot on the planets atmosphere that is offset from the sub-stellar point by westerly, equatorial winds (Showman & Guillot 2002; Knutson et al. 2007). The vertical rise of the phase curve therefore corresponds to the coming into view of that hot spot. Since it follows a sequence where methane is absent, by comparison, we can infer that there could be no methane absorption at

the hot spot, while remaining present in the surrounding regions.

Comparing HD 189733b’s magnitudes to a brown dwarf magnitude-spectral type relation (Dupuy & Liu 2012), a spectral type of L5 \pm 2 is expected on the dayside, and a spectral type of T5 \pm 3 on the nightside. The study of the L-T transition is an important research topic. At the transition, clouds that homogeneously cover L-dwarfs start breaking-up, revealing the deeper, hotter part of the atmosphere. This leads to a rapid change in J-H and J-K colours (Tinney, Burgasser & Kirkpatrick 2003; Vrba et al. 2004; Kirkpatrick 2005; Saumon & Marley 2008; Dupuy & Liu 2012). HD 189733b straddles the L-T transition. Future observations of the dayside in J, H and K bands would be particularly interesting to obtain in order to check whether the planet follows a sequence defined by young, directly imaged planets (Barman et al. 2011) or whether it behaves as field brown dwarfs do. If it does, we would expect a cloud cover on the dayside and a partly cleared weather on the nightside. A recent analysis of Kepler-7b’s phase curve demonstrated inhomogeneous cloud coverage can exist (Demory et al. 2013). This would imply that the transmission spectrum at ingress is likely different than at egress with repercussions on the current interpretation of such data. WASP-33b (Deming et al. 2012) and WASP-18b (Maxted et al. 2012) are marginally redder than the empirical M and L sequence. One could conclude their hot spot are also east of the substellar point, which is verified in WASP-18b’s case (Maxted et al. 2012).

Studying Figure 1 empirically informs that most *hot Jupiters* should be devoid of methane absorption on their illuminated hemisphere since most objects are located above the kink and follow the vertical M & L dwarf sequence. More measurements would be needed to observe whether there exists a distinction between the pM and pL classes were proposed by Fortney et al. (2008). Targets whose dayside emission is slightly cooler than HD 189733b, such as WASP-80b (Triaud et al. 2013a), will be of particular interest as they would presumably fall within the T range.

If carefully estimated, photometric distances can be accurately determined (e.g. Torres, Winn & Holman 2008). It would allow to complete those diagrams with the close to 40 systems that now have occultation measurements but do not have parallaxes (Triaud et al. in prep).

3 CONCLUSION

The launch of ESA's *GAIA* mission in December of this year will permit to increase the number of system with parallaxes. With additional systems we may start seeing the emergence of *planet families*. For example, we could check whether GJ 436 and HD 209458b are real outliers, or the first representatives of sub-classes of objects. Just like the compilation of the Hertzsprung-Russell diagram inspired theoretical developments in stellar evolution, theoretical sequences in colour-magnitude space could be computed for extrasolar planets. For known gravity, size and impacting flux, it may provide the means to distinguish different compositions and may even provide tests for the presence of an atmosphere, an ocean, or a surface (Selsis, Wordsworth & Forget 2011), which has implications in our eventual selection of suitable targets for the search for life on other worlds.

ACKNOWLEDGMENTS

This work originates from an inspiring discussion with Jackie Faherty in a sandwich shop in Santiago de Chile (called La Superior, on Nueva de Lyon), during which for the first time I really looked at a colour-magnitude diagram. I would like to thank Michael Gillon for reading over, to Heather Knutson for providing the phase curve data of HD 189733b, and to Nikole Lewis and Pierre Maxted for theirs. I would like to thank the anonymous referee for her/his comments that led to an improvement of the paper. I have made an extensive use of the exoplanet.eu (Schneider et al. 2011) and exoplanets.org (Wright et al. 2011) websites, as well of the NASA/ADS, Simbad and VizieR repositories.

This publication used data products from the Wide-field Infrared Survey Explorer, which is a joint project of the University of California, Los Angeles, and the Jet Propulsion Laboratory/California Institute of Technology, funded by the National Aeronautics and Space Administration. Data from the Two Micron All Sky Survey was also employed, which is a joint project of the University of Massachusetts and the Infrared Processing and Analysis Center/California Institute of Technology, funded by the National Aeronautics and Space Administration and the National Science Foundation.

I received funding under the form of a fellowship provided by the Swiss National Science Foundation under grant number PBGEP2-145594. During this fellowship, I am hosted by Joshua Winn, at the MIT Kavli institute and would like to thank him particularly, but also my colleagues for their welcome.

REFERENCES

Anderson D. R. et al., 2011, *ApJL*, 726, L19
 Baraffe I., Chabrier G., Allard F., Hauschildt P. H., 1998, *A&A*, 337, 403
 Barman T. S., Macintosh B., Konopacky Q. M., Marois C., 2011, *ApJ*, 733, 65
 Burrows A., Heng K., Nampaisarn T., 2011, *ApJ*, 736, 47
 Charbonneau D., Brown T. M., Latham D. W., Mayor M., 2000, *ApJL*, 529, L45

Chauvin G., Lagrange A.-M., Dumas C., Zuckerman B., Mouillet D., Song I., Beuzit J.-L., Lowrance P., 2004, *A&A*, 425, L29
 Cutri R. M., et al., 2012, *VizieR Online Data Catalog*, 2311, 0
 Deleuil M. et al., 2008, *A&A*, 491, 889
 Deming D. et al., 2012, *ApJ*, 754, 106
 Deming D., Seager S., Richardson L. J., Harrington J., 2005, *Nature*, 434, 740
 Demory B.-O. et al., 2013, *ApJL*, 776, L25
 Demory B.-O., Seager S., 2011, *ApJS*, 197, 12
 Díaz R. F. et al., 2013, *A&A*, 551, L9
 Dupuy T. J., Liu M. C., 2012, *ApJS*, 201, 19
 Fazio G. G. et al., 2004, *ApJS*, 154, 10
 Fortney J. J., Lodders K., Marley M. S., Freedman R. S., 2008, *ApJ*, 678, 1419
 Harrington J., Hansen B. M., Luszcz S. H., Seager S., Deming D., Menou K., Cho J. Y.-K., Richardson L. J., 2006, *Science*, 314, 623
 Kirkpatrick J. D., 2005, *ARA&A*, 43, 195
 Kirkpatrick J. D. et al., 2012, *ApJ*, 753, 156
 Knutson H. A., Charbonneau D., Allen L. E., Burrows A., Megeath S. T., 2008, *ApJ*, 673, 526
 Knutson H. A., Charbonneau D., Cowan N. B., Fortney J. J., Showman A. P., Agol E., Henry G. W., 2009, *ApJ*, 703, 769
 Knutson H. A., Charbonneau D., Noyes R. W., Brown T. M., Gilliland R. L., 2007, *ApJ*, 655, 564
 Knutson H. A. et al., 2012, *ApJ*, 754, 22
 Lépine S., Gaidos E., 2011, *AJ*, 142, 138
 Lewis N. K. et al., 2013, *ApJ*, 766, 95
 Luhman K. L., Burgasser A. J., Labbé I., Saumon D., Marley M. S., Bochanski J. J., Monson A. J., Persson S. E., 2012, *ApJ*, 744, 135
 Maeder A., 1974, *A&A*, 32, 177
 Marois C., Macintosh B., Barman T., Zuckerman B., Song I., Patience J., Lafrenière D., Doyon R., 2008, *Science*, 322, 1348
 Maxted P. F. L. et al., 2012, *ArXiv e-prints*
 Patten B. M. et al., 2006, *ApJ*, 651, 502
 Saumon D., Marley M. S., 2008, *ApJ*, 689, 1327
 Schneider J., Dedieu C., Le Sidaner P., Savalle R., Zolotukhin I., 2011, *A&A*, 532, A79
 Seager S., Deming D., 2010, *ARA&A*, 48, 631
 Selsis F., Wordsworth R. D., Forget F., 2011, *A&A*, 532, A1
 Showman A. P., Guillot T., 2002, *A&A*, 385, 166
 Southworth J., Wheatley P. J., Sams G., 2007, *MNRAS*, 379, L11
 Stevenson K. B. et al., 2010, *Nature*, 464, 1161
 Tinney C. G., Burgasser A. J., Kirkpatrick J. D., 2003, *AJ*, 126, 975
 Torres G., Winn J. N., Holman M. J., 2008, *ApJ*, 677, 1324
 Triaud A. H. M. J. et al., 2013a, *A&A*, 551, A80
 —, 2013b, *A&A*, 549, A18
 van Leeuwen F., 2007, *A&A*, 474, 653
 Vrba F. J. et al., 2004, *AJ*, 127, 2948
 Wright J. T. et al., 2011, *PASP*, 123, 412